Running title

A practical guide to starting SEM array tomography

Title

A practical guide to starting SEM array tomography – an accessible volume EM technique

Authors

Ian J. White and Jemima J. Burden

Affiliations

LMCB, University College London, London, WC1E 6BT, UK

Keywords

begin to acquire 3D ultrastructural data. With the addition of appropriate SEM-

therefore the sections not being in order; loss or damage to delicate sections at every ribbon split; loss of sections or sections ending up on non-imageable parts of the collection grid at each pick up stage; and damage to the delicate support film at any point between collection and imaging. Added to this fragility of process, the time to manually image every section, makes ssTEM an incredibly technically demanding, time and labour-intensive pursuit, and helps explain why as a technique it has generally been limited to smaller series and volumes. Longer series have been collected and imaged by particularly dedicated and experienced researchers, but generally with a very small blockface (30x150um for example) and still in the lower hundreds range (Cattin et al., 2015; Harris et al., 2006). This in part explains why much of the work on developing vEM sought to avoid the tricky sectioning and collection part of the process altogether, as well as automating the imaging. As backscatter electron SEM imaging improved to achieve closer to TEM ultrastructural resolution in biological samples, it created the possibility of developing SEM techniques to solve this problem. Focused Ion Beam (FIB, Pang et al MCB: Volume Electron Microscopy Volume 179) and Serial Blockface (SBF, Genoud et al MCB: Volume Electron Microscopy Volume 179) SEM both achieve this by imaging the blockface of the sample itself. Whilst solving many of the problems associated with ssTEM as described above, they introduce a new set of difficulties and limitations, such as being destructive one shot techniques precluding the ability to reimage samples, requiring alternative sample preps and resin embedding protocols, struggling to image bare resin areas without charging issues, and necessitating additional equipment such as an automated microtome to be added to the SEM chamber or having an expensive FIB in the SEM. Blockface techniques also require the user to start their imaging "blind", estimating where their ROI will appear in the block before it is eventually revealed by the cutting process, and where in X and Y it may subsequently go as imaging proceeds through the depth of the sample. SEM Array Tomography (SEM-AT) exists almost as a hybrid of these two approaches; a technique that avoids the new disadvantages of the blockface SEM techniques, and preserves the advantages of ssTEM whilst mitigating the difficulties described. Whilst certainly not without its problems and limitations, SEM-AT's hybrid approach allows it in w [(es)11 (u)11.6 (l)-4.3 (t)cace

Rationale

imaging in each section, whilst still allowing many hundreds of sections to be collected at once. The larger and less delicate collection substrate also means far fewer ribbon splits, section collection steps, and reduced risk of

can be reliably removed from the block between imaging (Chen et al., 2017; Wanner et al., 2015), and more significantly with FIB-SEM, where 4nm of the block can be milled away (Xu et al., 2017). Another potential disadvantage is the increased risk of introducing physical distortions in the sections during the mechanical cutting process, which can yield inaccuracies and require more post image acquisition processing to align the images into a smooth 3D volume.

The advantages, however, are significant and make it a particularly apt vEM choice for certain samples. The foremost of these is the non-destructive nature of the technique. Unlike SBF-SEM and FIB-SEM where the surface of the block is removed and destroyed/discarded before the blockface is imaged, and thus that material, no matter how interesting can never be re-imaged, SEM-AT allows the repeat imaging of sections. This can mean reimaging the same ROI at a different resolution, reimaging a different ROI in the same section set, reimaging regions of new interest that have only become apparent post the first round of acquisition, or reimaging for failed acquisition e.g. poor focus. Therefore, SEM-AT could be applied to precious samples eg. clinical biopsies, that need to be retained for future reference. A second major advantage is that all of the Z information is immediately laid out prior to high resolution imaging. The ability to capture a first round of lower resolution imaging, can greatly facilitate choice of final ROI and ROI tracking for structures that drift in X and Y, and/or meander through the depth of the sample. This allows the researcher to only image the sections and the area of each section where the ROI is present, increasing efficiency and throughput by saving significant amounts of time imaging, as well as reducing the overall dataset size – aiding downstream computational demands with alignments, analysis, sharing and storage. Thirdly, t

As such SEM-AT is a powerful, flexible, vEM technique that fills a niche for samples and imaging strategies that are not as well served by other vEM techniques.

KEY RESOURCES TABLE

Note that not all areas will be used in every protocol

REAGENT or RESOURCE	SOURCE	IDENTIFIER
Chemicals, Peptides, and Recombinant Proteins		
Chloroform	Fischer-Scientific	C/4960/PB08
Contact cement - DAP Weldwood	DAP	107
Poly-L-Lysine	Sigma	P 8920
Silver DAG	Agar Scientific	G3691
Triton X-100	Sigma	T8284
Xylene	TAAB	X001

MATERIALS AND EQUIPMENT

- Diamond knife suitable for ultrathin sectioning with large boat

- Single edge razor blades

- Trimming diamond (optional)

- Ultramicrotome with water withdrawal device

- SEM with array tomography software, sensitive backscatter electron detector, stage bias (ideal, but optional)

- SEM stubs, large enough for the ITO coverslips and compatible for the SEM stage

- Carbon stickies that are compatible with the SEM stubs

- Indium Tin Oxide (ITO) coated coverslips 22mm square, no.1.5 8-12ohms/sq

- Multi-meter to measure resistance

- Paint brush e.g. size 0 pure sable brush

- Eyelashes on cocktail sticks (three, one dedicated for use with contact cement)

- Silicon tubing to fit ultramicrotome water withdrawal device

- 10ml syringe

- Dispensing needle, short, blunt end, 14 gauge

- Paperclip large e.g. 5cm

- Pliers

- Sticky tape

- Permanent marker

- Ruler

- Forceps for handling coverslips

- Heat block suitable for 60°C.

BEFORE YOU BEGIN

Buffers/Materials to be made up in advance

- Contact cement -dilute contact cement with xylene, 1:1 (it shouldn't be stringy)

- Triton X-100- prepare a 0.1% solution with distilled water

- Poly-L-Lysine- prepare 1% and 0.1% solution with distilled water

- Silver DAG – dilute with manufacturer supplied diluent following manufacturer's instructions.

- Check and mark coverslips with a permanent marker so that ITO coated side 8 (er)-6.3 ( )]72.2 (r)l-12.2 (8 (er)-

into the knife and roughly position the paperclip to support the coverslip in such a way that the rear edge of the coverslip is resting on the back of the diamond knife boat, and out of the boat (Fig. 3B and C).

3. Secure the paper clip with two small pieces of tape, one on each side, taking care that the tape does not reach over the top edge of the boat (Fig. 3C).

4. Fill the boat with water and adjust level of the water so that the water is slightly concave at the knife edge. Then readjust the position of the coverslip (replacing the tape if necessary) so that the paperclip ensures that the coverslip sits stably in the boat, with the rear edge just slightly out of the water (Fig. 3B and C).

   Note: take note of where the water level reaches on the 22mm coverslip when the boat is filled with water to the correct level for sectioning. This indicates the line, up to which poly-L-lysine can be coated to aid section attachment at a later stage (Fig. 3D).

5. Once the paper clip is in the correct position, remove the water, clean the diamond, dry completely and store until needed.

6. To aid the collection of ribbons of the correct length, using a ruler and taking care not to touch the diamond, measure 18mm, horizontally back from the diamond, making a small mark on both sides of the knife boat (top edge) (Fig. 3E arrowhead).

[Insert Figure 3 here]

Prepare water withdrawal device on ultramicrotome

1. Connect one end of the silicone tubing to the water withdrawal device that comes with the microtome, as shown in Fig. 3F.

2. Connect the other end of the silicone tubing to a blunt dispensing needle. If necessary, wrap a little parafilm around to secure the connection.

3. Connect a 10 ml syringe that has been previously rinsed out several times with distilled water, to the dispensing needle.

Prepare ultramicrotome for serial sectioning

1. If possible, set up pre-set ultramicrotomy modes for:

    a. Ultrathin sectioning e.g. 70nm

    b. Ribbon splitting e.g. 5nm

A note about sample preparation

Unlike sample preparation for the blockface imaging techniques (FIB-SEM and SBF-SEM), sample preparation for array tomography is a little

size coverslip can support for example, ~600 ultrathin sections, from a blockface of dimensions ~ 1mm x 0.5mm. This represents a volume of ~21,000,000μm^3; 1000μm x 500μm x 42μm (assuming 70nm slices). It is recommended to be already proficient at ultrathin sectioning prior to attempting this protocol with precious samples and to ideally serial section in an environment free of vibration and drafts.

1. Using a single edge razor blade carefully trim to a blockface that is marginally larger than your ROI in X, Y and Z.
    a. leading and trailing edges must be parallel

            e   a

5. Take a 22mm ITO coverslip and dip 90% of the coverslip into 0.1% poly-l-lysine, leaving ~2mm uncovered, as shown in Fig. 3C, then place the coverslip, ITO side up, in the knife assembly.

    Glow discharging coverslips is another method for altering the hydrophobicity of the substrate.

6. Position the water withdrawal device on one side of the knife, positioning the end of the water withdrawal needle to the lowest point of the boat, angling the silicone tubing away from the user, Fig 3D. Secure the silicone tubing loosely with tape to the microtome body, Fig. 3F. This keeps it out of the way when cutting and reduces the chance of transferring vibrations to the boat water when removing water with the syringe.

7. Overfill the boat with filtered, distilled water, so that the level is slightly convex, but not overflowing, Fig. 3D. Use the syringe to withdraw water to the appropriate level for sectioning, e.g. slightly concave at the knife edge, Fig. 3E. Check the water interface at the edge of the coverslip. Ideally it will be flat, at 80-90% of the length of the coverslip. If necessary, use a paintbrush to "paint" a line of 0.1% poly-l-lysine at the top edge where the water/air interface will be, on the ITO side. Once satisfied, withdraw more water from the boat, so that the diamond knife is dry for alignment.

8. Align your block and diamond knife, using specimen rotation, knife rotation and specimen tilt to ensure that the knife is equidistant from the entire blockface.

9. Add water to the boat so that the water is slightly concave at the diamond knife and flat at the contact with the ITO, poly-l-lysine coated coverslip.

10. Optional: Add a single droplet of 0.1% Triton X-100 to the water to aid section handling.

11. Start ultrathin sectioning, taking care to observe the length of the ribbon, as it is produced, with respect to the 18mm ribbon length marker on the side of the knife boat, Fig. 3E arrowhead.

12. As the end of the ribbon approaches the 18mm mark, prepare to split the ribbon using one of the following methods (as shown in video 2):

    a. Quickly split the ribbon "on the fly" without pausing the cutting program, during the return stroke of the specimen arm.

b. Switch the sectioning mode to "5nm ribbon splitting" thickness for 2-3 cuts then return the ultramicrotome to "ultrathin sectioning" (personal communication, Rèza Shahidi).

c. Pause the cutting program during the return stroke and gently detach the ribbon from the diamond by dragging an eyelash over the diamond edge. Retract the sample by 200-500nm and restart the cutting program.

if using chloroform in step 17, take into account potential section expansion upon chloroform treatment, when predicting the length of your final ribbons.

13. An eyelash can be used to gently waft the first ribbon to the side of the boat, out of the way of the next ribbon.

14. Steps 12 and 13 can be repeated numerous times until several ribbons have been collected. After the sample has passed the knife edge, pause the cutting. Use eyelashes to gather and dock these first ribbons to each other, side by side, in the correct order. This reduces the chance of ribbons getting mis ordered later. method (lhs)-12.)i)34tonersevveris12.3 l3.1 (t(7(n)-p ()-12.2 af)-1.1 har

a fast and sensitive backscatter detector to image sections rapidly at low kV to prevent sample damage. Focus, stigmation and stage movement must be automated and accurate, mosaic stitching must be possible to provide coherent pictures of large areas, tools to define individual sections and further define ROI for imaging must exist, and preferably this all has to be brought together in one user friendly software package.

The following protocol describes the general principles and workflow of SEM-AT imaging irrespective of imaging equipment specification/manufacturer used. However, some details given are specific to our system which is: Zeiss Gemini 300 FEG SEM-AT high vacuum with SENSE backscatter electron detector and Tandem Decel stage bias system, using ATLAS 5 software for automated array tomography image acquisition.

Firstly, set up basic parameters to achieve high quality images on an unimportant part of a sample before further imaging. This will be sample and microscope dependent, however, the following are factors to consider:

- Set the sample to a working distance optimized for the backscatter detector as advised by microscope manufacturer.

- Adjust beam voltage to obtain a satisfactory image without inducing beam related damage/artefacts.

- Adjust pixel dwell/imaging time to achieve an optimum signal to noise ratio without inducing charging effects/sample movement/darkening.

- Adjust brightness and contrast to suit.

Optimizing imaging parameters can be a protracted but worthwhile process, and an optimised protocol for one sample can be a good starting point for optimisation on a similar sample. In our system we begin with an accelerating voltage of 4.5kV reduced to a landing energy of 1.5kV via a 3kV stage bias, and tailor the pixel dwell time according to resolution required for the particular type of imaging (0.2-2μs per pixel).

Once optimised, the rest of the process is performed in specific array tomography software, be it ATLAS 5 in Zeiss, Maps in Thermo Fisher Scientific, SEM Supporter/SEMography in Jeol or ACAT in Hitachi systems, for example.

The initial image acquisition stage requires mapping of the ribbons in their entirety into the array tomography software. This is achieved by drawing a bounding box around the section ribbons and utilizing a high speed low resolution imaging protocol e.g. 600nm pixel size and sub microsecond pixel dwell time without auto functions, (video 4). Ribbon outlines for bounding box positioning are ascertained either by live image, alignment of multiple SEM visualised points with an existing optical camera image, or by SEM still images of outer ribbon extremities. The final aim is to visualise with sufficient resolution to show individual section boundaries, and rouirautceb3 (l)3.2(er)-6.3 (8 (i)3.1 (ETJ24.22402 0 Td5

damaged edges and therefore modified section outlines. In these circumstances an alternative method involves defining a rectangle, aligning the long edge parallel with the section leading or trailing edge to achieve correct rotation, and then placing the centre of this rectangle on a feature constant throughout the array, (Fig. 5C), which requires sufficient resolution. After initial ribbon mapping, it may be necessary to map the sections at a higher resolution, for example 200nm pixel size, to visualise an appropriate feature, this is also beneficial to accurate section placement by the automated systems and is often necessary for identification of sample features for later selection of ROI. Whilst accurate manual section marker placement and/or fine adjustment o(d i)3.2 h9 (e h9 (e.337 0 Td[(F)-5 (t)-1

Usually, ROI markers of different geometries are available. It is worth considering at this point the advantage of limiting the numb

of view comprised of millions of pixels, and image series over hundreds of sections, so the minimal time without compromising on image quality should be selected, with perhaps a small margin to account for imaging differences between sections.

Any image requiring mosaic tiling will have an impact on acquisition time as overlapping areas have to be imaged, and software stitching of tiles must take place. If possible, it is wise to avoid/minimize the need for tiling. This can be achieved through a variety and/or combination of mechanisms, e.g. altering ROI shape and/or size, where the current size or shape goes just over the threshold requiring extra tiles; or by a small change in pixel size, where this allont ter2(ha)2.2 (l)3cixel sd equ-1.1 (er)-6

Image alignment

feature transform (SIFT) methods, using texture and features in the images as references, caution should be taken when aligning data with features that collectively track across the dataset in X or Y, or collectively spiral. This is to avoid artificially straightening the data. If possible, including features that migrate through the Z stack in multiple directions, will minimize this risk. Regardless of what alignment strategies are used, resulting aligned stacks should be "sense checked" by carefully observing the stack, scrolling first through the XY planes, and then XZ and YZ planes. Ultimately, any small inaccuracies or mis-alignments can often be manually corrected, prior to cropping the dataset and 3D reconstruction/analysis.

Discussion and advances

Array tomography is a non-destructive EM approach that provides 3D ultrastructural information of cells and organelles at nm resolution across mi2 r0.2. seals romscstestEana9(t)3J(r)-9.o(is)-11(u(t)3J (

SEM for easier correlation and re-location of ROI (Burel et al., 2018; Micheva & Smith, 2007).

Prospects and future challenges:

Improvements in the areas of serial sectioning and collection are lowering the entry barrier for researchers wanting to take advantage of the potential of SEM-AT. In addition, with SEM-AT imaging being a software solution rather than requiring specialist hardware, SEM-AT is becoming an increasingly cost-effective, flexible and attractive prospect for those wishing to enter the field of vEM. Nevertheless, there remain challenges to be solved and improvements made, to enable everyday users to exploit the technique to its fullest potential.

Currently, it is relatively straightforward to collect hundreds of serial sections using the basic manual techniques we have described above. With the attention being given to this area, as demonstrated by the development of the automated techniques and of knife/knife boat modifications, it is likely that we will continue to see improvements, both commercial and "lab hacks", to make it more user friendly and accessible to less experienced microtomists. Whilst obviously crucial, sectioning and collection is a relatively small part of the SEM-AT process in terms of time expenditure, thus the real gains to be made are in the field of imaging. Whilst still not quite at the level of TEM, the resolution and image quality of section imaging on a modern, appropriately equipped, SEM has proven easily sufficient for answering most cell biology research questions, e.g. imaging membranes, virus, membrane contacts, synaptic vesicles etc (Collman et al., 2015; Kataoka et al., 2019; Norris & Terasaki, 2021; Terasaki et al., 2013). Further improvements will undoubtedly be made, but as of this time the ultimate resolution of imaging is not the decisive factor when considering SEM-AT in most projects, rather it is the time taken to acquire the images that is the limiting step. Currently all systems require significant user input, early in the process. Whilst not technically demanding, furtherg

analysis challenges associated with the information dense vEM data, - for which many research

Burel, A., Thérèse Lavault, M.-T., Clément Chevalier, C., Gnaegi, H., Prigent, S., Mucciolo, A., Dutertre, S. S., Humbel, B. M., Guillaudeux, T., & Kolotuev, I. (2018). A targeted 3D EM and correlative microscopy method using SEM array tomography https://doi.org/10.1242/dev.160879

Cardona, A., Saalfeld, S., Schindelin, J., Arganda-Carreras, I., Preibisch, S., Longair, M., Tomancak, P., Hartenstein, V., & Douglas, R. J. (2012). TrakEM2 software for neural circuit reconstruction. PLoS ONE, 7(6). https://doi.org/10.1371/JOURNAL.PONE.0038011

Carl Zeiss Microscopy GmbH. (2020). High Resolution and High Throughput Imaging of Tissue Samples Using The ATLAS™. AZoNano. https://www.azonano.com/article.aspx?ArticleID=2724

Cattin, A. L., Burden, J. J., van Emmenis, L., MacKenzie, F. E., Hoving, J. J. A., Garcia Calavia, N., Guo, Y., McLaughlin, M., Rosenberg, L. H., Quereda, V., Jamecna, D., Napoli, I., Parrinello, S., Enver, T., Ruhrberg, C., & Lloyd, A. C. (2015). Macrophage-Induced Blood Vessels Guide Schwann Cell-Mediated Regeneration of Peripheral Nerves. Cell, 162(5), 1127–

de Schepper, S., Ge, J. Z., Crowley, G., Ferreira, L. S. S., Garceau, D., Toomey, C. E.,

Sokolova, D., Childs, T., Lashley, T., Burden, J. J., Jung, S., Sasner, M., Frigerio, C. S., &

Hong, S. (2022). Perivascular SPP1 Mediates Microglial Engulfment of Synapses in

Alzheimer's Disease Models. BioRxiv, 2022.04.04.486547.

https://doi.org/10.1101/2022.04.04.486547

Analysis of Cells from Lung Autopsy Specimens following Fatal A/H1N1 2009 Pandemic Influenza Virus Infection. Journal of Virology, 93(19). https://doi.org/10.1128/JVI.00644-19

Koike, T., Kataoka, Y., Maeda, M., Hasebe, Y., Yamaguchi, Y., Suga, M., Saito, A., & Yamada, H. (2017). A Device for Ribbon Collection for Array Tomography with Scanning Electron Microscopy. Acta Histochem. Cytochem., 50(5), 135–140. https://doi.org/10.1267/ahc.17013

Kruit, P., & Zuidema, W. (2019). A Dedicated Multi-Beam SEM for Transmission Imaging of Thin Samples. Microscopy and Microanalysis, 25(S2), 1034–1035. https://doi.org/10.1017/S1431927619005907

Lee, T. J., Yip, M. C., Kumar, A., Lweallen, C. F., Bumbarger, D. J., Reid, R. C., & Forest, C. R. (2020). Capillary-and Stokes-based trapping of serial sections for scalable 3D-EM connectomics. ENeuro, 7(2). https://doi.org/10.1523/ENEURO.0328-19.2019

Li, X., Ji, G., Chen, X., Ding, W., Sun, L., Xu, W., Han, H., & Sun, F. (2017). Large scale three-dimensional reconstruction of an entire Caenorhabditis elegans larva using

Peddie, C. J., Genoud, C., Kreshuk, A., Meechan, K., Micheva, K. D., Narayan, K., Pape, C.,
Parton, R. G., Schieber, N. L., Schwab, Y., Titze, B., Verkade, P., Weigel, A., &
Collinson, L. M. (2022). Volume electron microscopy. Nature Reviews Methods
Primers, 2(1), 51. https://doi.org/10.1038/s43586-022-00131-9

Schalek, R., Kasthuri, N., Hayworth, K., Berger, D., Tapia, J. C., Morgan, J. L., Turaga, S. C.,
Fagerholm, E., Seung, H. S., & Lichtman, J. W. (2011). Development of High-
Throughput, High-Resolution 3D Reconstruction of Large-Volume Biological Tissue
Using Automated Tape Collection Ultramicrotomy and Scanning Electron
Microscopy. Microscopy and Microanalysis, 17(2), 966.
https://doi.org/10.1017/S1431927611005708

Schindelin, J., Arganda-Carreras, I., Frise, E., Kaynig, V., Longair, M., Pietzsch, T.,
Preibisch, S., Rueden, C., Saalfeld, S., Schmid, B., Tinevez, J. Y., White, D. J.,
Hartenstein, V., Eliceiri, K., Tomancak, P., & Cardona, A. (2012). Fiji: An open-source
platform for biological-image analysis. Nature Methods, 9(7), 676–682.
https://doi.org/10.1038/NMETH.2019

Spomer, W., Hofmann, A., Veith, L., & Gengenbach, U. (2020). Chapter 5 A Low-Tech
Approach to Serial Section Arrays. Volume Microscopy: Multiscale Imaging with
Photons, Electrons, and Ions, Neuromethods, 155. https://doi.org/10.1007/978-1-
0716-0691-9_5

Stalling, D., Westerhoff, M., & Hege, H.-C. (2005). amira: A Highly Interactive System for
Visual Data Analysis | Elsevier Enhanced Reader. Visualization Handbook.

Started, G., Images, A., Alignment, M. I., Alignment, A. I., Information, G. Q., & Topics, S. H.

Zuidema, W., & Kruit, P. (2020). Transmission imaging on a scintillator in a scanning electron microscope. Ultramicroscopy, 218, 113055. https://doi.org/10.1016/J.ULTRAMIC.2020.113055

Figure Legends:

Figure 1: Summary of the described SEM-AT workflow.

A) Preserved, heavy metal contrasted sample is embedded in a resin block and mounted for trimming. B) Asymmetric ultrathin sections, with parallel leading and trailing edges, form a neat ribbon during sectioning. C) Multiple ribbons split into suitable lengths are collected in sequence order on an ITO coated coverslip to form an array of many hundred sections. D) Coverslip is mounted onto an

A) A metal paperclip is "unfolded", trimmed to appropriate length depending on knife width and moulded to shape using pliers. B) End view shows the paperclip folded over the edges of the knife boat on both sides and running across the bottom of the trough. The side view shows the paperclip positioned such that when the collection substrate is inserted into the knife boat, the lower edge rests stably against the paperclip at the bottom of the trough, and the upper edge protrudes from the water by 1-2mm and rests against the rear edge of the knife boat. C) A photo of the apparatus shows the

Video Captions:

Video 1: Contact cement application

Video 2: Section splitting

Video 3: Water withdrawal and section collection

Video 4: Ribbon scans

Video 5: Automated section marking

Figures:
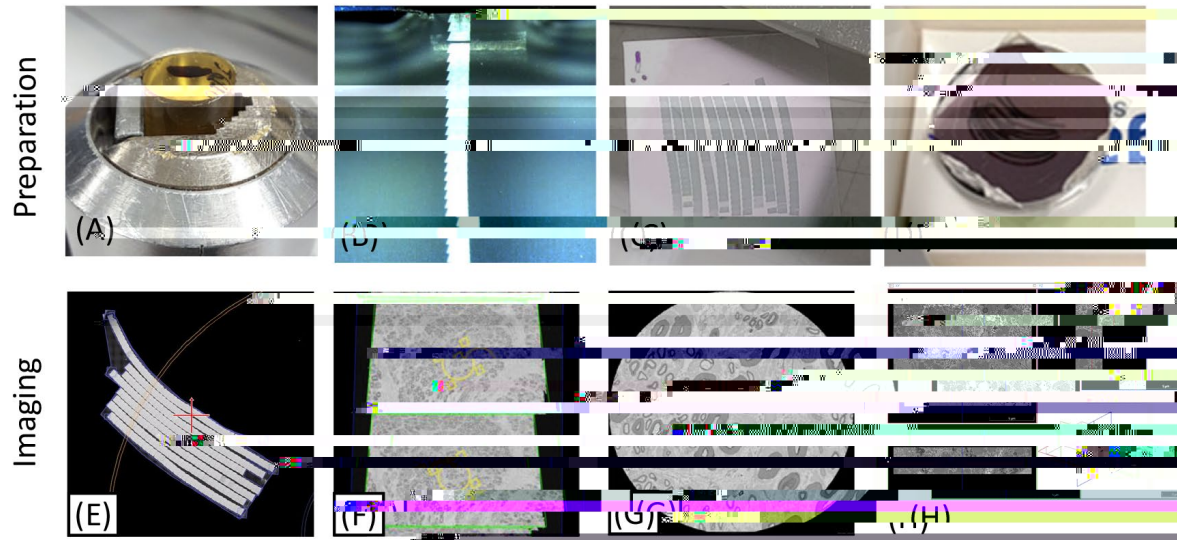
Figure 1: Summary of the described SEM-AT workflow.

Figure 2: Comparison of the ssTEM and SEM-AT workflows.

Figure 3: Simple modifications to the knife and microtome for inexpensive and easy collection of arrays of hundreds of sections on coverslips.
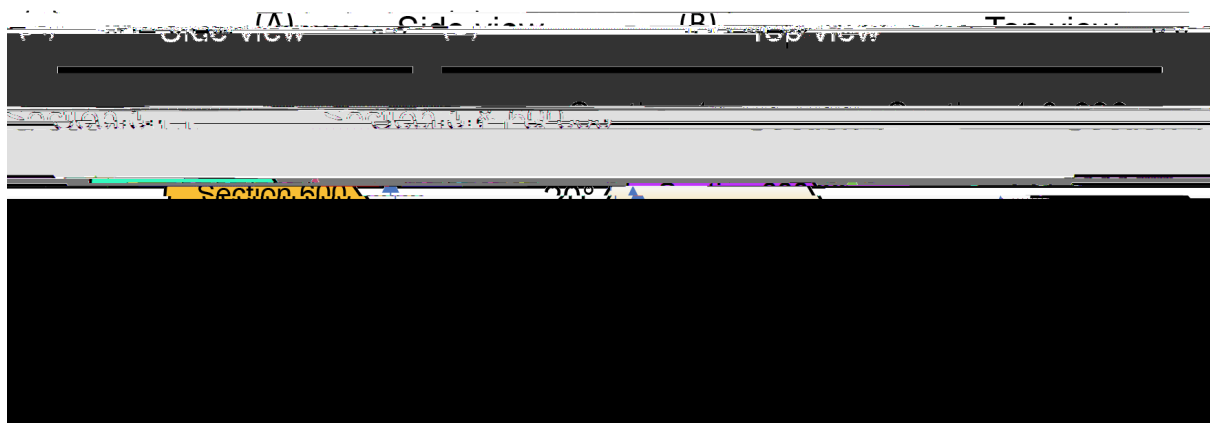
Figure 4: Geometry of blockface preparation: impact upon serial section sizes

Figure 5: Section and ROI defining methods